Efficient spin injection in graphene using electron optics

H. Y. Tian, K. S. Chan,* and J. Wang†
Department of Physics, Southeast University, Nanjing, 210096, China and
Department of Physics and Materials Science, City University of Hong Kong, Tat Chee Avenue, Kowloon, Hong Kong, China
(Received 7 October 2012; published 14 December 2012)

We investigate theoretically spin injection efficiency from the ferromagnetic graphene to normal graphene (FG/NG) based on electron optics, where the magnetization in the FG is assumed from the magnetic proximity effect. Based on a graphene lattice model, we demonstrated that one spin-species electron flow from a point source could be nearly suppressed through the FG-NG interface, when the total internal reflection effect occurs with the help of an additional barrier masking the Klein tunneling, while the opposite spin-species electron flow could even be collimated due to the negative refraction under suitable parameters. Not only at the focusing point is the efficient spin injection achieved, but in the whole NG region the spin injection efficiency can also be maintained at a high level. It is also shown that the nonideal FG-NG interface could reduce the spin injection efficiency since the electron optics phenomena are weakened owing to the interfacial backscattering. Our findings may shed light on making graphene-based spin devices in the spintronics field.

DOI: 10.1103/PhysRevB.86.245413 PACS number(s): 85.75.−d, 72.25.Hg, 73.40.Gk, 81.05.ue

I. INTRODUCTION

Since the successful fabrication of a single layer of graphite in laboratory, graphene has become one of the central research activities in condensed matter physics, nanotechnology, and material science disciplines.[1–3] Graphene is an one-atom-thick layer of carbon atoms tightly packed into a honeycomb crystal lattice whose symmetries lead to a linear energy-momentum relation for the low-energy quasiparticles, which can be described by the massless relativistic Dirac equation. Owing to its unique band structure and linear energy dispersion, the bulk graphene can exhibit many peculiar properties such as Klein tunneling,[4] specular Andreev reflection,[3] and unconventional half-integer quantum Hall effect.[5]

Graphene is also a particularly promising material for application to spintronics because it is expected to have a very long spin-diffusion length due to its weak spin-orbital and hyperfine interactions.[6–8] Similar to the semiconductor-based spin devices, the principal challenge in making graphene-based spin devices is to realize efficient spin injection from a spin resource to graphene. Plenty of experimental works[9–11] have been implemented and the spin injection efficiency (SIE) is not as large as that expected from theoretic calculations because of the conductivity mismatch between a ferromagnetic metal and graphene. To overcome it, the tunnel barriers such as Al_2O_3 or MgO, by using the molecular beam epitaxy or atomic layer deposition technique, were grown between ferromagnetic metal and graphene, and significant improvement of SIE was observed in recent experiments.[12,13]

At theoretic aspects, some novel proposals[14–16] were also put forward to enhance the SIE by means of the unique properties of graphene, for example, Moghaddam and Zareyan[16] proposed in a normal/ferromagnetic/normal graphene (NG/FG/NG) device to use the graphene Veselago lens effect[17–19] to collimate one spin-species electrons and realize a high spin polarization at the focal point. Since at the low-energy regime, the quasiparticles in graphene have a linear energy dispersion just like photons, and the electron and hole have opposite chiralities, the negative refraction Klein tunneling could occur in a *pn* graphene interface. In the FG/NG junction, one spin-species channel can be electrically modulated as a *pn* junction as long as the ferromagnetic exchange energy is larger than the Fermi energy. However, it is fairly difficult for applications to the graphene-based spintronics, though the high spin polarization could be achieved at the focusing point. On the one hand, the Veselago lens effect in graphene is crucially dependent on a precise parameter value and the spin polarization denoting the SIE can even reverse at places slightly away from the focal point; on the other hand, the focusing effect can be weakened when the FG-NG interface is nonideal and the backscattering is present, so the SIE at the focal point would be depressed.

To overcome the weakness of such spin lens effect used to realize a high SIE, we propose to use another phenomenon of electron optics, the total internal reflection at the FG-NG interface, to suppress one spin-species electron flow so as to enhance the SIE. Similar to the E-M waves scattering at the dielectric interfaces, the quasiparticles passing through the FG-NG interface need to conserve their transverse momenta, so that a larger Fermi momentum mismatch between FG and NG can lead to a smaller critical incident angle, below which the transmission is allowed, and vice versa. By introducing an additional tunnel barrier[20] blocking the normal incidences and electrically varying the local Fermi energies, one can realize simultaneously to block one spin-species electron transport and collimate the opposite spin-species electron flow in the NG region. Meanwhile, the linear E-k relation of the low-energy particles in graphene makes the electron trajectories nondispersive over a finite energy window imposed by bias and temperature.

In this work we theoretically study the SIE from the FG into NG by means of the electron optics phenomena of quasiparticles, and the electrons are injected into the FG by a point source and collected in the NG by a drain electrode. The uniform ferromagnetism in the FG is assumed to stem from the magnetic proximity effect with a magnetic insulator supporting graphene as shown in Fig. 1(a). Based on a tight-binding lattice model, we demonstrated both the focusing effect and total reflection effect of electron flow through the FG-NG interface.

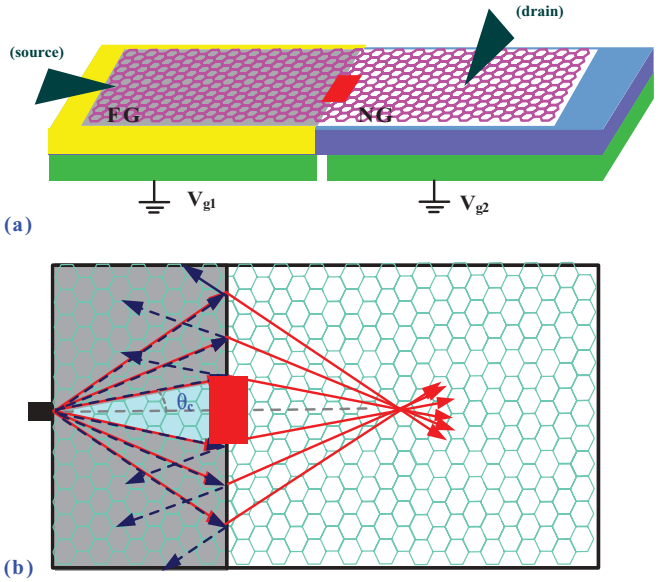

FIG. 1. (Color online) (a) Plot of a schematic two-terminal graphene device. Gate voltage V_{g1} and V_{g2} can control the local potentials of FG and NG, respectively; a point source angularly spreads electrons while an extended drain collects those that refract around the tunnel barrier made from a lattice void. (b) Trajectories of the spin-up electrons (red solid-line arrows) that are collimated due to negative refraction and spin-down electrons (blue dotted-line arrows) that are totaly reflected with the help of a tunnel barrier.

It is shown that by modulating electric gate voltages, one spin-species electron flow is experiencing the focusing effect, whereas the opposite spin channel exhibits the total internal reflection effect, as a result, a high SIE is achieved almost in the whole NG region not limited to the focal point. When a smooth FG-NG interface is considered, the high SIE is slightly suppressed in comparison with the sharp interface case.

The rest of the paper is organized as follows. In Sec. II we model the FG/NG junction in the tight-binding representation, and then present the formulas to calculate the local particle density as well as the spin polarization. In Sec. III the numerical results and discussions of enhancing SIE are given. Finally, a brief summary is presented in the last section.

II. MODEL AND FORMALISM

A two-terminal FG/NG device is schematically shown in Fig. 1(a), where the left semi-infinite graphene nanoribbon is deposited on a magnetic insulator that can induce the exchange field h in the FG region, while the right one is the NG on a normal nonmagnetic substrate. The source electrode injects electrons into the FG and the drain electrode in the NG collects them. The two gate voltages V_{g1} and V_{g2} can, respectively, control the local chemical potentials in the FG and NG, and determine the carrier types, holelike or electronlike. For the FG, two spin channels may have the opposite chiralities when the exchange energy h is larger than the Fermi energy E_F, so that the focusing and total internal reflection effects may simultaneously appear in the circuit. A rectangular lattice void[20] with width d and length l is engineered at the FG-NG interface to block the nearly perpendicular incidence of electrons from the source, which makes it possible to block one spin-species electron flow as illustrated in Fig. 1(b).

We employ a lattice model in the tight-binding representation to describe the system

$$H = \sum_{l\sigma}(U_j + \sigma h)C^\dagger_{l\sigma}C_{l\sigma} - \sum_{\langle lm\rangle\sigma} t(C^\dagger_{l\sigma}C_{m\sigma} + \text{c.c.}) + \sum_{\alpha,k\sigma}[\varepsilon_{\alpha,k\sigma}d^\dagger_{\alpha,k\sigma}d_{\alpha,k\sigma} + (\gamma C^\dagger_{\mathbf{l}\alpha\sigma}d_{\alpha,k\sigma} + \text{c.c.})], \quad (1)$$

where the first and second terms describe the graphene ribbon, $C^\dagger_{l\sigma}(C_{l\sigma})$ is the creation (annihilation) operator at site l with spin σ ($\sigma = \pm = \uparrow\downarrow$), $\langle lm\rangle$ denotes the summation over the nearest-neighbor sites, t is the hopping integral, U_j stands for the lattice site energies of the FG ($j = F$) and NG ($j = N$) region, which are controlled by gate voltages V_{g1} and V_{g2}, respectively; h is the exchange field in the FG region and vanishes in the NG. The last term in the above equation refers to the source and drain electrodes described in the k space with spin σ and their couplings to the graphene lattices $\mathbf{l}_\alpha$, where α ($\alpha = s,d$) represents the source and drain electrodes, and $d_{\alpha,k\sigma}(d^\dagger_{\alpha,k\sigma})$ is the annihilation (creation) operator of the electrons in the electrode α with spin σ.

As usual, the SIE is denoted by the spin polarization of the source-drain conductance and defined as

$$P = \frac{G_\uparrow - G_\downarrow}{G_\uparrow + G_\downarrow}, \quad (2)$$

where $G_{\uparrow(\downarrow)}$ denotes the spin-up (spin-down) conductance of the system. In terms of the nonequilibrium Green's function technique, the spin-dependent current flowing to the drain electrode can be expressed as

$$J_\sigma = \frac{e}{h}\int dE\{T_\sigma(E)[f_d(E) - f_s(E)]\}, \quad (3)$$

where T_σ is the spin-dependent electron transmission from the source to drain electrodes, and $f_{s(d)}(E)$ is the Fermi distribution function of the source (drain) electrode that is assumed in local equilibrium. In the linear transport regime and at zero temperature, the spin-resolved conductance is reduced to

$$G_\sigma = \frac{e^2}{h}T_\sigma(E_F) = \frac{e^2}{h}Tr[\Gamma_d G^r \Gamma_s G^a]_{\sigma\sigma}, \quad (4)$$

where $\Gamma_{s(d)}$ is the linewidth function of the source (drain) electrode and in the wide-band approximation,[21] $\Gamma_{s(d)} = i(\Sigma^r_{s(d)} - \Sigma^a_{s(d)}) = 2\pi\gamma^2\rho_{s(d)}(E_F)$ with $\rho_{s(d)}$ being the Fermi density of states of the source (drain) electrode and $\Sigma^r_{s(d)}$ ($\Sigma^a_{s(d)}$) being the corresponding retarded (advanced) self-energy; G^r (G^a) is the retarded (advanced) Green's function and given by

$$G^r(E) = \left[E\sigma_0 - \tilde{H} - \Sigma^r_s - \Sigma^r_d\right]^{-1}, \quad (5)$$

where σ_0 is a unit matrix, $\tilde{H}$ is the first two terms of Eq. (1) by excluding the source and drain electrodes as well as the couplings, which are considered through the self-energies in the above equation. Actually, the semi-infinite FG and NG are also denoted by the lead self-energies and the matrix dimension of G^r is determined by the lattice span between the source and drain electrodes. Note that the two spin channels

are independent since there is no spin noncollinearity taken into account.

To demonstrate the electron optics phenomenon in graphene like the Veselago lens effect, one usually considers the response of the local particle density to the electron injected from the source electrode as done in Refs. 16 and 19. Actually, in the small bias limit, the variation of the local particle density per voltage $\delta\rho_\sigma(l)$ is given by

$$\delta\rho_\sigma(l) = \frac{e^2}{2\pi}\mathrm{Tr}[G^r\Gamma_s G^a]_{l\sigma l\sigma}, \tag{6}$$

where the trace, the same as that in Eq. (4), is over the local lattice sites coupling with the drain electrode. Obviously $\delta\rho$ is proportional to the local conductance G_σ in Eq. (4) when the coupling strength γ between the drain electrode and graphene lattice is a constant, so that the Γ_d is a unit matrix. This is exactly the assumption of the wideband approximation. As a result, the local density variation is proportional to the local conductance distribution and both of them can display the trajectories of the injected wave packets' evolution in the FG/NG junction.

In the following calculations we set both the source and drain electrodes coupling with a single unit cell of honeycomb lattice, and the obtained particle density variation $\delta\rho_\sigma$ and spin polarization P could be renormalized to represent the original six discrete sites of a hexagon, that is, these quantities will be plotted in a rectangular lattice that is mapped from the honeycomb lattice. This scheme was also adopted in Ref. 19 to display the focusing effect of electrons in the graphene pn ribbon junction.

III. RESULTS AND DISCUSSION

According to the formulas presented in the last section, we shall in this section calculate numerically the local particle density variation $\delta\rho_\sigma$ as well as the spin polarization P, which are induced by the injected electrons from the source electrode. The spin polarization P can stand for the SIE in the studied FG/NG system. As stated earlier, the linear E-k relation of particles at low energy together with the pseudospin property give the carriers in graphene a pseudorelativistic chiral nature, that is, the electron and hole have different chiralities so that an electronic version of the Veselago lens is expected in a pn graphene junction. An electronic wave packet emitted from a point $x = (-a,0)$ in the n-type region shall be focused at the point $x' = -xk_n/k_p$ in the p-type region with k_n (k_p) being the Fermi momenta in the n-type (p-type) region. Certainly this analysis in the continuum model is based on the assumptions of the sharp pn interface and no intervalley scattering.

When the electronic wave packet is scattered at the interface of the graphene junction like nn^+ or pp^+ not limited to pn, the conservation of the transverse momenta $k_F \sin\theta_1 = k_N \sin\theta_2$ defines a critical incident angle, beyond which the electronic wave will be totally reflected, where k_F (k_N) is the Fermi momenta at the left (right) side of the junction interface, and θ_1 (θ_2) is the incident (transmitted) angle. In the calculations, the hopping energy is taken as $t = 2.75$ eV, the temperature is set $T = 0$ K, the global Fermi energy is set as $E_F = 0$, and the nearest-neighbor and the next nearest-neighbor carbon-carbon bonds are respectively set as $a = 0.142$ nm and $b = \sqrt{3}a \simeq 0.25$ nm as in a real graphene sample. In following discussions, the sharp interface is assumed otherwise stated explicitly between the FG and NG regions.

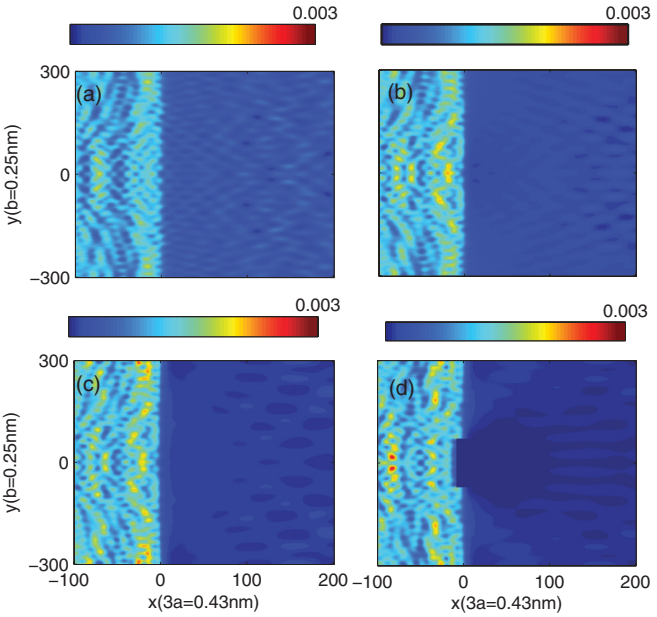

FIG. 2. (Color online) Distribution of local particle density variation $\delta\rho_\downarrow(l)$ in an armchair FG/NG nanoribbon junction for $U_N = -0.1t$ in (a), $U_N = -0.07t$ in (b), and $U_N = -0.04t$ in (c) and (d). A tunnel barrier is considered in (d) with the barrier width $d = 150b$ and length $l = 20 \times 3a$. Other parameters are the ribbon width $W = 601b$, the source position is $(-250 \times 3a,0)$, $h = 0.1t$, and $U_F = -0.06t$.

In Figs. 2 and 3 we plot the evolution processes of the total reflection for the spin-down carriers in the lattice FG/NG junction, where both the armchair-edge (Fig. 2) and zigzag-edge (Fig. 3) nanoribbons were calculated. As is seen, the $\delta\rho_\downarrow$ in the NG region denoting the transmitted waves become weaker and weaker, when the local potential U_N decreases gradually and the Fermi momentum k_N in the NG decreases correspondingly. Meanwhile, the reflections are enhanced with U_N since the critical incident angle decreases, $\theta_c = \sin^{-1} k_N/k_{F\downarrow}$, where $k_{F\downarrow}$ is the spin-down Fermi momentum in the FG region. However, the perpendicular injection from the FG into NG cannot be prohibited unless the Fermi momentum $k_N = 0$, which implicates zero density of states at the Fermi level. In order to block entirely small-angle incident carriers from the source, a tunnel barrier, which could be an engineered lattice void, should be introduced at the FG-NG interface. The calculated results are shown in Figs. 2(d) and 3(d), and it is seen that the transmitted waves are almost vanishing or at least negligibly small in comparison with those cases without the barrier in Figs. 2(c) and 3(c). In other words, the spin-down channel is nearly in the OFF state owing to the manufactured total internal reflection effect on the FG-NG interface.

One shall not try to close the spin-down channel in the NG by modulating the local electrostatic potential so as to realize $k_N = 0$, because at the same time, the spin-up channel is also closed due to vanishing density of states in the NG. More importantly, the particle transport in reality is always allowed in a finite energy window imposed by temperature or

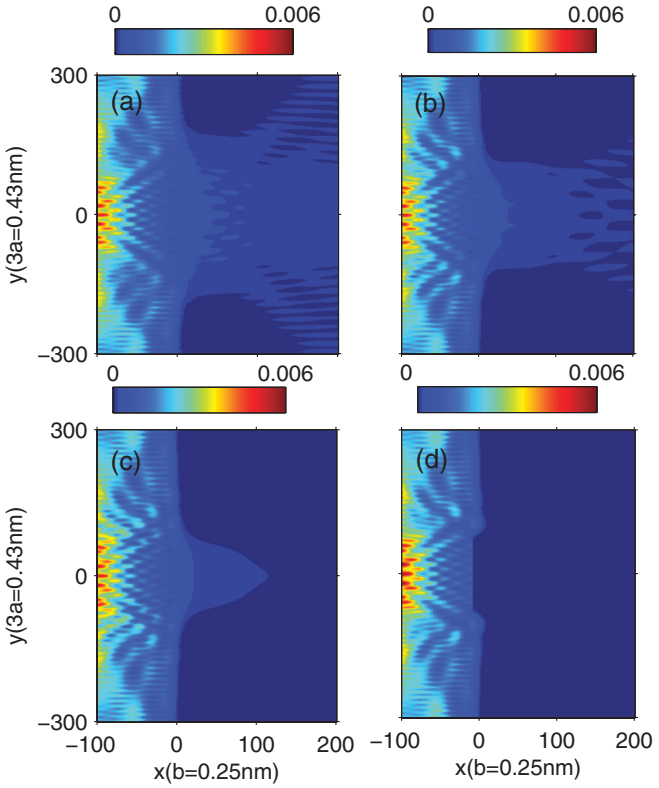

FIG. 3. (Color online) Distribution of local particle density variation $\delta\rho_{\downarrow}(l)$ in an zigzag FG/NG nanoribbon junction. Parameters are exactly the same as the armchair ribbon case shown in Fig. 2.

source-drain bias, therefore, it is meaningless to block the particle transport by using the zero density of states at the Dirac point in graphene. Furthermore, the electron-hole puddles[22] in the realistic graphene lattice prohibit one to approach precisely the Dirac point. It is also seen that there is not much difference for the total reflection effect between the armchair-edge (Fig. 2) and zigzag-edge (Fig. 3) FG/NG junction, and the reflection in the zigzag-edge nanoribbon seems clearer than that in the armchair-edge case owing to the presence of small refraction near the barrier in Fig. 2(d). This is different from the Veselago lens effect in the graphene *pn* junction studied in Ref. 19, in which the armchair-edge *pn* junction was shown to exhibit a perfect focusing effect since only intraband scattering occurs at the interface. Similarly, it is this intraband scattering that makes the transmitted waves in the NG region more homogeneous in the armchair-edge nanoribbon (Fig. 2) than the zigzag-edge one (Fig. 3). Therefore, we will focus on enhancement of the SIE in the armchair-edge nanoribbon by introducing the total internal reflection at the FG-NG interface since it is expected that the zigzag-edge ribbon should be more efficient for SIE than the armchair-edge one.

The spin-up carriers in the FG region $U_F + h > 0$ are holelike while they are electronlike in the NG region with $U_N < 0$, the opposite chiralities shall lead to the negative refraction effect for those spin-up carriers at the FG-NG interface. In Fig. 4 we present such focusing contour for the spin-up channel in the armchair-edge FG/NG junction with the same parameters used in Figs. 2 and 3. When the tunnel barrier of lattice void is considered, one can see that the

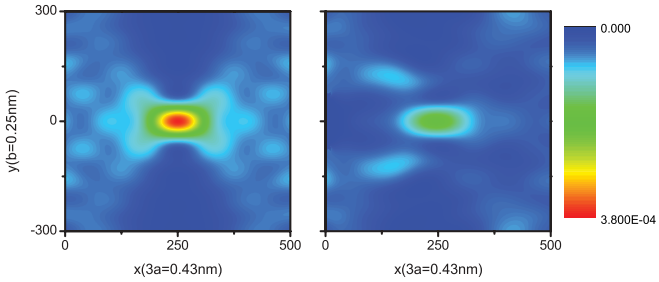

FIG. 4. (Color online) Distribution of spin-up particle density variation $\delta\rho_{\uparrow}(l)$ in the FG/NG armchair-edge nanoribbon junction without a barrier (a) and with a barrier (b). Parameters are same as with those in Fig. 2.

focusing pattern does not vanish but the focusing strength becomes weaker, because the nearly perpendicular (small angle) incidence has a larger Klein transmission and dominates the focusing effect.

Two spin channels are independent in the FG/NG junction, so the focusing effect and total reflection effect in each spin channel may simultaneously appear by modulating the local potentials U_F and U_N. The focusing effect in the spin-up channel does not play a decisive role in our scheme to enhance the SIE from the FG to the NG since the efficient SIE is feasible as long as the total reflection occurs and blocks the spin-down carriers. In Fig. 5 we plot the spin polarization P distribution in the NG region. It is seen that the SIE is high only at the focal point in the absence of the tunnel barrier in the junction [Figs. 5(a) and 5(c)], and the spin polarization can even be reversed when the drain electrode deviates from the focal point. As is expected, the spin polarization P can be maintained at a high level in the whole NG regions when the tunnel barrier is introduced at the FG-NG interface [Figs. 5(b) and 5(d)]. We have also studied the case of the smooth interface between the FG and NG, in which the linear variation of the magnetization h and electrostatic potential $U_F - U_N$ is considered within the

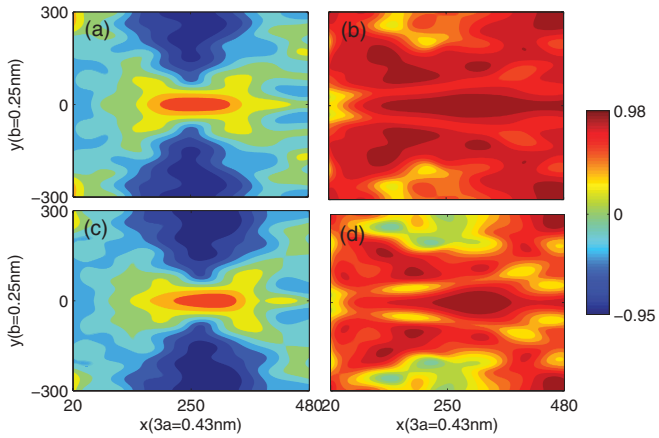

FIG. 5. (Color online) Spin polarization P in the armchair-edge FG/NG junction without a barrier in (a) and (c), and with a barrier in (b) and (d). A smooth FG-NG interface was considered in (c) and (d) instead of the sharp interface in (a) and (b). Parameters are the ribbon width $W = 601b$, the source position at $(-250 \times 3a, 0)$, $h = 0.1t$, and $U_F = -0.06t$, $U_N = -0.04t$, the barrier width $d = 127b$, and length $l = 20 \times 3a$.

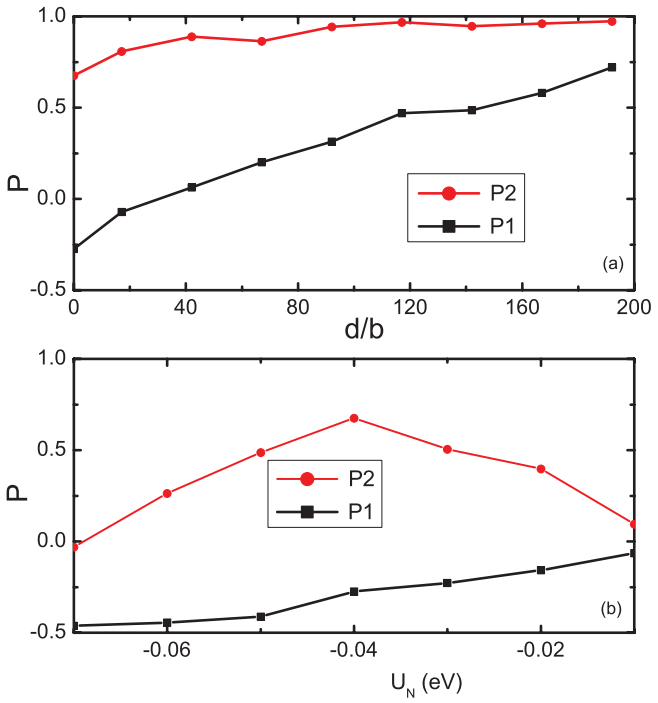

FIG. 6. (Color online) Spin polarization P_1 and P_2 in the armchair-edge FG/NG junction as a function of the barrier width d in (a) and the local potential U_N. The lattice size is the width $W = 601b$ and length $450 \times 3a$ in the NG region. Parameters are $h = 0.1t$, $U_F = -0.06t$, and $U_N = -0.04t$ in (a), $d = 0$ in (b).

barrier length l. Such nonideal interface can weaken both the focusing effect and total reflection effect due to the presence of backscattering, so the spin polarization is also reduced a little as shown in Figs. 5(c) and 5(d). Even so, the average SIE can be kept on a high level in comparison with that only resulting from the focusing effect.

In Fig. 6 we proceed to examine the barrier width dependence of the spin polarization P_1 and P_2, which denote, respectively, the average spin polarization over all the NG regions and the spin polarization at the focal point. It is shown that P_1 increases linearly with the increase of the width d since the spin-down channel was gradually closed. Oppositely, the focal spin polarization P_2 is kept at a high level and increases a little. As is expected, when the total reflection occurs, the average polarization P_1 should exhibit a saturation value $P_1 \simeq 0.48$ at the critical barrier width $d_c = 2L \tan(\theta_c) \approx 127b$, which is denoted by the platform in Fig. 6(a). The further increase of P_1 at $d > d_c$ may relate to the definition of the SIE that would increase when both two spin-species conductances decrease owing to the increase of the tunnel barrier strength, which is an usual method to enhance the SIE from the ferromagnetic metals into semiconductors by using a tunnel barrier. In Fig. 6(b) P_1 and P_2 are plotted as a function of the local potential U_N in the absence of the tunnel barrier. It is clearly shown that the P_2 can reach its maximum at an unique parameter value $U_N = -(U_F + h)$ so that the spin-up carriers can be precisely collimated through the negative refraction effect, whereas the average spin polarization P_1 maintains a negative value. Therefore, only focusing effect in the FG/NG junction shall not be an efficient way to enhance the SIE.

IV. CONCLUSION

In conclusion, we have demonstrated numerically the electron optics phenomena, the Veselago lens effect and total internal reflection effect in a single FG/NG nanoribbon junction. By use of these two effects, we found that an efficient spin polarization can be obtained in the NG region by using a point source injecting electrons into FG, because one spin-species channel could be nearly closed due to the total internal reflection at the FG-NG interface with the help of an introduced tunnel barrier, while the opposite spin-species carriers can even exhibit the focusing effect by controlling the local potentials. The high SIE is thus achieved not only at the focal point but also in the whole NG region. It is also found that a sharp FG-NG interface is desirable for the graphene electron optics and the SIE.

ACKNOWLEDGMENTS

We are very grateful to J. T. Song and Y. X. Xing for helpful correspondence. This work was supported by the General Research Fund of the Research Grants Council of Hong Kong SAR, China (Project No. CityU100311/11P) and NSFC (Grant Nos. 11274260, 11274059, 11074032). J.W. also acknowledges support from 973 Project of China (2009CB929504).

*apkschan@cityu.edu.hk
†jwang@seu.edu.cn

[1] K. S. Novoselov, A. K. Geim, S. V. Morozov, D. Jiang, Y. Zhang, S. V. Dubonos, I. V. Grigorieva, and A. A. Firsov, Science **306**, 666 (2004).
[2] Y. Zhang, Y. W. Tan, H. L. Stormer, and P. Kim, Nature (London) **438**, 201 (2005).
[3] C. W. J. Beenakker, Rev. Mod. Phys. **80**, 1337 (2008).
[4] M. I. Katsnelson, K. S. Novoselov, and A. K. Geim, Nat. Phys. **2**, 620 (2006).
[5] D. A. Abanin, P. A. Lee, and L. S. Levitov, Phys. Rev. Lett. **96**, 176803 (2006).
[6] C. L. Kane and E. J. Mele, Phys. Rev. Lett. **95**, 226801 (2005).
[7] O. V. Yazyev, Nano Lett. **8**, 1011 (2008).
[8] K. I. Bolotin, K. J. Sikes, Z. Jiang, G. Fudenberg, J. Hone, P. Kim, and H. L. Stormer, Solid State Commun. **146**, 351 (2008).
[9] S. Cho, Y.-F. Chen, and M. S. Fuhrer, Appl. Phys. Lett. **91**, 123105 (2007).
[10] N. Tombros, C. Jozsa, M. Popinciuc, H. T. Jonkman, and B. J. van Wees, Nature (London) **448**, 571 (2007).
[11] W. Han, W. H. Wang, K. Pi, K. M. McCreary, W. Bao, Y. Li, F. Miao, C. N. Lau, and R. K. Kawakami, Phys. Rev. Lett. **102**, 137205 (2009).

[12] W. Han, K. Pi, K. M. McCreary, Y. Li, J. J. I. Wong, A. G. Swartz, and R. K. Kawakami, Phys. Rev. Lett. **105**, 167202 (2010).
[13] T. Yamaguchi, S. Masubuchi, K. Iguchi, R. Moriya, and T. Machida, J. Mag. Mag. Mater. **324**, 849 (2012).
[14] I. J. Vera-Marun, V. Ranjan, and B. J. van Wees, Phys. Rev. B **84**, 241408(R) (2011).
[15] D. A. Abanin, R. V. Gorbachev, K. S. Novoselov, A. K. Geim, and L. S. Levitov, Phys. Rev. Lett. **107**, 096601 (2011).
[16] A. G. Moghaddam and M. Zareyan, Phys. Rev. Lett. **105**, 146803 (2010).
[17] V. V. Cheianov, V. Fal'ko, and B. L. Altshuler, Science **315**, 1252 (2007).
[18] A. Yamakage, K. I. Imura, J. Cayssol, and Y. Kuramoto, Phys. Rev. B **83**, 125401 (2011).
[19] Y. X. Xing, J. Wang, and Q. F. Sun, Phys. Rev. B **81**, 165425 (2010).
[20] R. N. Sajjad and A. W. Ghosh, Appl. Phys. Lett. **99**, 123101 (2011).
[21] A. P. Jauho, N. S. Wingreen, and Y. Meir, Phys. Rev. B **50**, 5528 (1994).
[22] J. Martin, N. Akerman, G. Ulbricht, T. Lohmann, J. H. Smet, K. V. Klitzing, and A. Yacoby, Nat. Phys. **4**, 144 (2008).